UNIVERSIDADE DE LISBOA
FACULDADE DE CIÊNCIAS
DEPARTAMENTO DE BIOLOGIA ANIMAL

A large scale analysis of the dynamic cell behaviours that underlie the growth of the zebrafish posterior body

Fernando António Vinagre Duarte

Dissertação
Mestrado em Biologia Evolutiva e do Desenvolvimento
2014

UNIVERSIDADE DE LISBOA
FACULDADE DE CIÊNCIAS
DEPARTAMENTO DE BIOLOGIA ANIMAL

A large scale analysis of the dynamic cell behaviours that underlie the growth of the zebrafish posterior body

Fernando António Vinagre Duarte

Dissertação orientada por:
Doutora Estelle Hirsinger
Professora Doutora Sólveig Thorsteinsdóttir

Dissertação
Mestrado em Biologia Evolutiva e do Desenvolvimento
2014

Acknowledgements

“For the night is dark and full of terrors”

- George R. R. Martin

Even if fictional and unusual, I start this section with this quote as it captures quite well this period of my life. Not the writing up of this dissertation, but life as a whole. On that note, I would like to give my special thanks to my friend Joana Carvalho. For being there both during the good (and I must admit there were not many), the bad and specially the ugly moments. We started this journey together and oh girl we know how long and difficult it turned out to be. We have seen each other growing up so much, and the same way you were my rock throughout this past two years, I will be there for you if and when the time comes.

A special thanks to Florian Fabre too, for providing the extra kick of energy and inspiration when I was needing it the most. Let’s hope it wasn’t too little, too late, and that three years from now we will be celebrating yet one more phase of our lives. Get ready!

For not letting me sink and helping me to get back to my feet, I dedicate this dissertation to you two with love. This obviously extends to all my friends and family; I am grateful for all your sacrifices and for always being there for me.

For cultivating my interest in Science from an early point of my life, and later in Developmental Biology, a big thanks to my cousin Fernanda Bajanca and to my supervisor Professor Sólveig Thorsteinsdóttir, respectively.

Last but not least, I finish with a special thanks to my two supervisors in Paris, Estelle Hirsinger and Ben Steventon, for taking me as their student, for making my adaptation to Paris so smooth, for their exemplar professionalism and for all the scientific advice they provided me, not only regarding the project but about Science and research in general. To Ben for all I know about microscopy and image analysis, and for all your enthusiasm, fun conversations and cool ideas on zebrafish tailbud elongation. I hope to succeed in Science one day and show you two all your hard work in forming me was worth it.

Abstract

As vertebrate embryos develop, their posterior axis undergoes marked changes in size and tissue architecture. The morphogenetic behaviours underlying the formation of the posterior trunk and tail are complex. As of today, two models for posterior body formation have been proposed: the blastema and the "continuity of gastrulation" model. These two models can be rationalised into two canonical morphogenetic processes: the blastema model proposing that posterior body elongation is driven by anisotropic growth, whereas the continuation of gastrulation model postulates it is driven by tissue deformations. To address the relative contribution of these two mechanisms on posterior body elongation, we captured confocal stacks of fixed zebrafish embryos at different developmental stages, labelled with nuclear and membrane markers and performed surface reconstructions of all the posterior segments to measure their dimensions. Our morphogenetic analysis revealed not only that tailbud outgrowth undergoes at least two distinct phases, the first dominated by tissue deformation, the second by growth, but also that the majority of growth seems to occur in the anterior segments. Furthermore, we developed retrospective clonal analysis, a genetic single-cell labelling technique, in the zebrafish embryo, to investigate the identity and growth modes of the posterior axis precursors. With this method, we found no evidence of the existence of a stem cell pool resident in the zebrafish tailbud, which lead us to believe that posterior body formation in this model must be driven mainly by proliferation/dispersion of lineage-restricted progenitors. This observation was supported by the results we obtained while monitoring cell cycle progression in tailbud cells in Cecyil fish, a zebrafish transgenic line harbouring a set of cell cycle markers coupled with different fluorescent molecules, where we could not detect persistent proliferation in the tailbud.

Keywords: Zebrafish tailbud elongation | Anisotropic growth | Tissue deformation | Morphometric analysis | Retrospective clonal analysis

Resumo

O alongamento de tecidos desempenha um papel crucial durante a morfogénese. Para além de desempenhar um papel directo ao proporcionar forma aos tecidos, na maioria dos casos a falha deste processo resulta numa panóplia de defeitos na morfogénese. Um exemplo claro disso pode ser observado em anomalias existentes na formação do tubo neural tanto em *Xenopus* (Wallingford and Harland, 2012), como no ratinho (Ybot-Gonzalez *et al.*, 2007), e mesmo no humano (Kibar *et al.*, 2007). Além disso, também foi demonstrado que defeitos no alongamento estão implicados no aparecimento do lábio leporino, um dos defeitos congénitos mais observados em humanos (Parker *et al.*, 2010). O alongamento da região posterior do corpo após a gastrulação é um dos exemplos mais marcáveis de alongamento de tecidos durante o desenvolvimento embrionário. Ao passo que a região anterior do corpo se desenvolve a partir de células que migram durante a gastrulação, num processo denominado ingressão (Kinder *et al.*, 1999), a região posterior do tronco e a cauda formam-se a partir de um grupo de progenitores localizados na extremidade posterior do embrião numa região denominada botão caudal. Apesar desta ser uma região bastante restrita em termos de dimensões no embrião, ela é responsável pela formação de dois terços da porção posterior do eixo antero-posterior (Kanki and Ho, 1997).

No decorrer do último século, o estudo do desenvolvimento do corpo dos vertebrados tem sido objecto de controvérsia, devido à incerteza em relação à conservação dos mecanismos responsáveis pela formação da região anterior e posterior do corpo (Handrigan, 2003). Neste contexto, duas visões opostas de como o crescimento posterior ocorre foram propostas. Uma delas (Holmdahl, 1925) propõe que o botão caudal consiste numa amálgama homogénea de células indiferenciadas, ou blastema, caracterizada pela combinação de uma elevada taxa de proliferação aliada à capacidade de gerar vários tipos de tecidos ao longo do eixo antero-posterior. Além disso, este modelo sugere igualmente que o crescimento do botão caudal ocorre na ausência de movimentos celulares tipicamente observados durante a gastrulação, e que, ao invés disso, tem lugar através de desenvolvimento secundário, à semelhança daquilo que ocorre durante o desenvolvimento do botão do membro. Contrariamente, a outra (Pasteels, 1943) propõe a noção oposta, ou seja, defende que a formação da região

posterior do corpo resulta apenas da continuação dos processos iniciados durante a gastrulação, que incluem uma série de movimentos celulares.

Tendo em conta ambos os modelos, é possível imaginar que o alongamento da região posterior do corpo pode ser explicado através de crescimento anisotrópico (proposto pelo modelo do blastema de Holmdahl), de deformações no tecido (proposto pelo modelo de continuação da gastrulação de Pasteels), ou pela combinação de ambos.

Avanços recentes nas ferramentas disponíveis para realizar estudos de *imaging*, como por exemplo a utilização de técnicas modernas de microscopia confocal para realizar vídeos em tempo real, possibilitam a aquisição de *datasets* contínuos durante um longo período de tempo, permitindo a análise de comportamentos e movimentos morfogenéticos a nível celular. Juntamente com o aparecimento de *software* de análise de imagem mais poderoso, neste momento temos acesso a uma panóplia de métodos de alta resolução que nos permitem analisar o crescimento do embrião. Neste sentido, uma espécie opticamente transparente que possua desenvolvimento externo, e que portanto é facilmente acessível para qualquer tipo de manipulação, como é o caso do embrião de peixe-zebra, é especialmente indicada para este tipo de estudos. Por este motivo, seleccionámos o peixe-zebra como organismo modelo para utilizar neste estudo.

Com o objectivo de analisar os comportamentos e movimentos morfogenéticos que ocorrem ao nível do tecido dos segmentos posteriores do embrião de peixe-zebra, e assim determinar a contribuição relativa dos dois mecanismos de crescimento do botão caudal referidos anteriormente, realizámos uma série de experiências, incluindo análises morfométricas, análise clonal retrospectiva e monitorização em tempo real do ciclo celular de células progenitoras residentes no botão caudal. Desta forma, no presente estudo pretendemos analisar: (1) as dimensões (comprimento, largura e altura) e o volume dos segmentos posteriores de embriões de peixe-zebra entre os estadios de 10 sómitos (14 *hpf*) e 32 sómitos (25,4 *hpf*), recorrendo à utilização do *software* Imaris; (2) as divisões celulares que ocorrem no botão caudal através da monitorização em tempo real do desenvolvimento da região posterior em embriões de peixe-zebra transgénicos da linha Cecyil, que possuem uma série de marcadores do ciclo celular acoplados a moléculas fluorescentes que permitem acompanhar a progressão do ciclo celular em células progenitoras residentes no botão causal; (3) as características (dimensões, frequência, identidade, distribuição e modo de crescimento) dos nichos de células progenitoras residentes ao nível do botão caudal, a partir dos clones gerados através da

técnica de análise clonal retrospectiva, que se baseia na marcação aleatória e hereditária de células individuais, permitindo a análise clonal dos seus descendentes a longo prazo (Petit *et al.*, 2005).

A nossa análise morfométrica permitiu-nos identificar duas fases distintas envolvidas no processo de alongamento da região posterior do corpo no peixe-zebra. A primeira fase (em embriões com 14 a 21 *hpf*, ou seja, de 14 a 24 somitos) caracteriza-se por um aumento relativamente lento do comprimento e volume do embrião acompanhado por uma diminuição na largura e aumento na altura, sugerindo que o crescimento anisotrópico e apenas moderado e que a principal causa por detrás do alongamento provem de deformações do tecido, ao passo que a segunda fase (em embriões a partir de 21 *hpf*) é caracterizada por um aumento rápido do comprimento e do volume acompanhado pela estabilização da largura e altura dos segmentos, o que indica a ocorrência de apenas pequenas alterações na forma do tecido em conjunto com um crescimento anisotrópico acentuado. De um modo geral, estes resultados sugerem um cenário onde diferentes processos se encontram em jogo em alturas específicas e críticas do desenvolvimento para promoverem o alongamento do botão caudal.

Tendo em conta estes resultados, e de forma a determinar quais os segmentos posteriores onde crescimento anisotrópico de facto ocorre, decidimos analisar variações no volume ao longo do tempo em todos os segmentos posteriores do embrião, a partir dos sómitos 13-14 até ao botão caudal, em embriões do estádio de 10 (14 *hpf*) até ao estadio de 30 somitos (24,4 *hpf*). Esta análise permitiu-nos concluir que crescimento anisotrópico mais acentuado ocorre maioritariamente nos segmentos que se encontram mais distanciados do botão caudal e que correspondem aos sómitos que se formam em primeiro lugar no embrião em todos os estadios de desenvolvimento. Após monitorização cuidadosa dos embriões durante alongamento do botão caudal, dois processos biológicos destacaram-se como bons candidatos hipotéticos para explicar esta resposta por parte do tecido, sendo eles o processo de dilatação das células da notocorda e a miogénese, mais especificamente o alongamento de miofibrilhas ao longo dos sómitos. Por este motivo, decidimos determinar em cada estadio do desenvolvimento qual o ultimo segmento posterior onde estes dois processos são observáveis, e comparar estas observações com as variações de volume observadas anteriormente em todos os segmentos posteriores.

Por fim, propusemo-nos a analisar quais os modos de crescimento (baseado em proliferação/dispersão *vs*. nicho de células progenitoras estaminais) em jogo durante o alongamento do botão caudal. Como ponto de partida, os nossos resultados utilizando a linha Cecyil de peixe-zebra demonstraram que não existem praticamente células em proliferação activa no botão caudal, ou seja, na fase S do ciclo celular, o que sugere que o botão caudal não possui um nicho de células progenitoras estaminais. Estes resultados foram ainda corroborados pela nossa análise clonal retrospectiva, uma vez que que ao analisármos a biblioteca de clones obtida não conseguimos identificar nenhum clone multipotente que poderia sugerir a existência de um nicho de células estaminais residente no botão caudal.

Apesar do nosso estudo ter já providenciado pistas em relação aos mecanismos e modos de crescimento envolvidos no processo de alongamento do botão caudal em peixe-zebra, futuramente seria importante realizar mais estudos focados na análise dos mecanismos celulares e moleculares responsáveis pela regulação deste processo, tais como: (1) analisar os comportamentos celulares por detrás das alterações observadas ao nível do tecido em relação à forma e tamanho dos segmentos; (2) investigar o papel que tanto a dilatação das células da notocorda como o alongamento das miofibrilhas ao longo dos sómitos desempenham durante o alongamento da região posterior do corpo de um modo mais detalhado; (3) confirmar a importância do papel da proliferação celular durante este processo, bem como a (não)existância de um nicho de células estaminais residentes no botão caudal em peixe-zebra; (4) realizar estudos complementares em diferentes organismos, incluindo amniotas e anamniotas, como por exemplo o anfioxo, de forma a efectuar estudos comparativos com o objectivo de estudar a conservação, ou não, dos mecanismos evolutivos por detrás do alongamento do botão caudal.

Palavras-chave: Alongamento do botão caudal em peixe-zebra | Crescimento anisotópico | Deformação do tecido | Análise morfométrica | Análise clonal retrospectiva

Table of Contents

I. Introduction

Tissue elongation is a crucial event in morphogenesis. Besides its direct role in shaping tissues, elongation failure is thought to be the cause of many common morphology defects. For one, failure of dorsal tissue elongation has been implicated as the main cause of neural tube defects in both frog (Wallingford and Harland, 2012), mouse (Ybot-Gonzalez *et al.*, 2007) and human (Kibar *et al.*, 2007). Elongation failure is also known to be implicated in one of the most common congenital birth defect in humans, the cleft palate (Parker *et al.*, 2010).

One of the most striking examples of tissue elongation during development is the elongation of the posterior body following gastrulation. Whereas the anterior trunk arises from cells that ingress during gastrulation (Kinder *et al.*, 1999), the posterior trunk and tail tissues form from a group of progenitors located in the posterior most end of the embryo in a region called the tailbud. Despite of being restricted to a small region of the embryo, this region generates the posterior two thirds of the body axis (Kanki and Ho, 1997).

Recent advances of tools for imaging, such as live imaging using modern confocal microscopy techniques, grant us the opportunity to capture continuous long-term data-sets of morphogenetic behaviours. Together with the advent of more powerful image analysis software, we now have the methods for high-resolution analysis of growth. Optically transparent and easily accessible species (*i.e.* species that develop externally), such as the developing zebrafish embryo, are especially well suited for such analysis.

I.1. Gastrulation in Zebrafish

Vertebrate gastrulation comprises a set of stereotypical cell movements that will ultimately lead to the formation of the three germ layers – endoderm, mesoderm and ectoderm – responsible for generating every tissue and organ present in the adult (Kanki and Ho, 1997; Montero and Heisenberg, 2004). Gastrulation in zebrafish starts as epiboly movements that are the migration of blastodermal cells over the yolk cell towards the vegetal pole of the embryo (Kanki and Ho, 1997; Montero and Heisenberg, 2004). Meanwhile, ingression movements taking place at the margin of the blastoderm

will lead to the internalization of mesendodermal progenitor cells that will form the hypoblast layer and will later give rise to the mesoderm and endoderm germ layers (Kimmel *et al.*, 1990; Montero and Heisenberg, 2004). All the ectodermal and neuroectodermal derivatives present in the embryo will arise from the non-internalized superficial cells remaining in the epiblast layer (Kimmel *et al*., 1990; Shih and Fraser, 1995). Cells of the epiblast and hypoblast will then converge to the future dorsal side of the embryo and undergo convergence extension, ultimately resulting in the narrowing and extension of the embryo body along the medio-lateral and anterior-posterior axes, respectively (Kanki and Ho, 1997; Montero and Heisenberg, 2004).

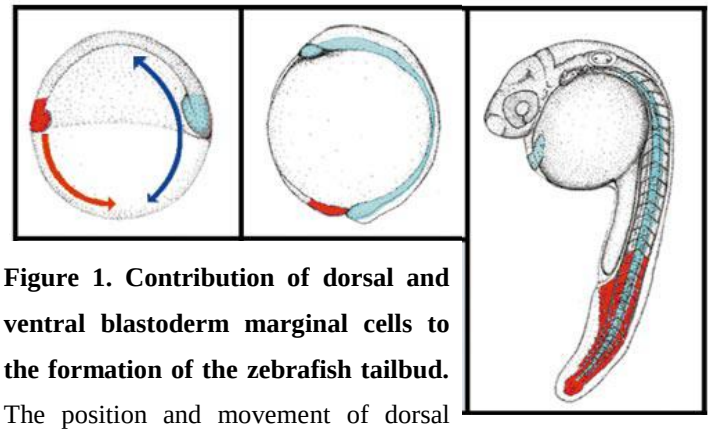

Figure 1. Contribution of dorsal and ventral blastoderm marginal cells to the formation of the zebrafish tailbud. The position and movement of dorsal (blue) and ventral (red) blastoderm marginal cells at the shield stage (left panel), by the end of gastrulation (central panel) and at 24 *hpf* (right panel).

As seen in Agathon *et al*., 2003

I.2. Posterior body elongation in zebrafish

At the end of gastrulation, the tailbud starts to form as the cells of the blastoderm margin come together, fusing with each other over the ventral yolk cell (Westerfield, 1993; Kimmel *et al*., 1995). Whereas ventral marginal cells slip over the yolk plug, giving rise to the posterior half of the tailbud, the dorsal marginal cells migrate further, extending towards the animal pole and originate the anterior half (Kanki and Ho, 1997; Agathon *et al*., 2003) (Fig.1). According to Kanki and Ho, this constitutes the first stage of zebrafish posterior body formation occurring between 11 and 12 *hours post-fertilization* (*hpf*). During the second stage, the tailbud extends along the ventral side of the yolk (between 12 up to17 *hpf*), stopping once it reaches the midpoint along the ventral side. During the third stage (from 17 to 18 *hpf*), cells accumulate at the extremity of the tailbud forming a larger protruding aggregate. Once the tailbud undergoes the fourth stage of eversion and detaches itself from the yolk (from 18 *hpf* onward), the extending appendage is designated as the developing tail (Fig.2).

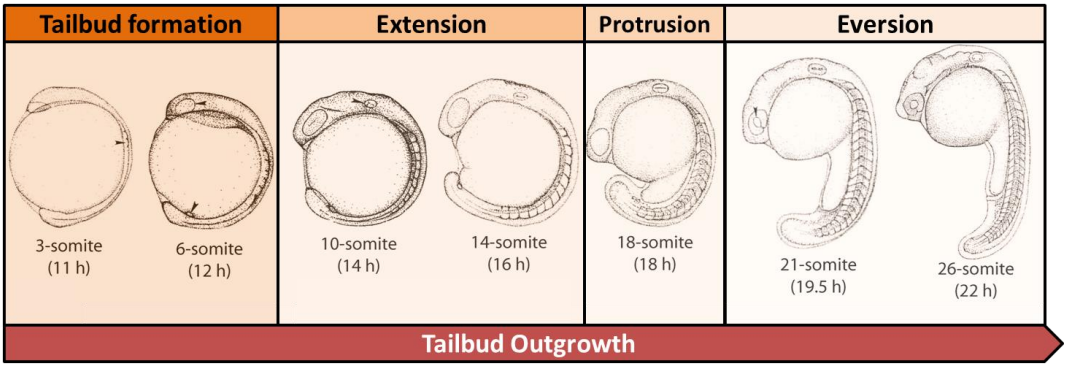

Figure 2. Zebrafish posterior body formation throughout development. The four distinct phases leading to tail formation are indicated above. The developmental stages (in somite number and *hpf*) are shown below each embryo panel.

Adapted from Kanki and Ho, 1997 and Kimmel, 1995

I.3. Tailbud modes of growth

The study of vertebrate body development has generated controversy over the past century and led to a longstanding question on whether the mechanisms underlying anterior and posterior body formation are the same (Handrigan, 2003). Two extreme views of posterior growth have been proposed. One view (Holmdahl, 1925) proposed that the tailbud is a homogeneous mass of undifferentiated cells or blastema, characterized by the combination of a high proliferation rate and the capacity to generate all tissue types along the entire posterior axis. In addition, it is suggested that tailbud outgrowth occurs in the absence of the cell movements typically observed during gastrulation and takes place through secondary development, in a manner that is comparable to limb bud development (see Model 2 in Fig.3). The other view (Pasteels, 1943) proposed the opposite notion, arguing that posterior body formation is a simple continuation of the processes initiated during gastrulation, which includes cell relative movements (see Model 1 in Fig.3). According to Pasteels view, the three germ layers are established during gastrulation.

In zebrafish, time-lapse imaging (Kanki and Ho, 1997) revealed that tailbud outgrowth involves, to some extent, the gastrulation movements responsible for head and anterior trunk patterning, such as convergence-extension. There are in addition novel posterior-specific cell movements, such as subduction and lateral divergence. The restricted fate view is supported by lineage tracing experiments showing that the tailbud contains distinct domains restricted to specific cell fates (Kanki and Ho, 1997). However, it is important to keep in mind that possibly this fate map missed the existence of

multipotent precursors, owing to the small number of labelled cells. Fate map studies are not exhaustive because only a small fraction of the cells are labelled, which does not allow for the identification of rare events such as the existence of stem cell pools.

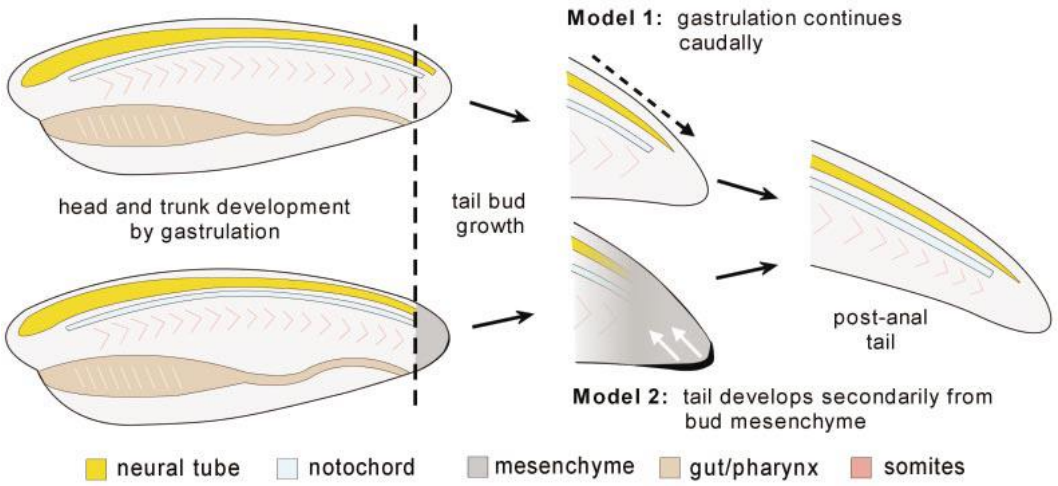

Figure 3. Vertebrate tailbud outgrowth. According to **Model 1**, morphogenetic movements (*i.e.* gastrulation) occurring within the head and trunk of the embryo continue beyond the anus (dashed arrows), resulting in tailbud formation. On the other hand **Model 2** states that tailbud outgrowth does not rely on the morphogenetic movements typically observed during gastrulation and arises instead from secondary inductive events, regulated by morphogenetic signals (white arrows) emanating from a thickened homogeneous region located at the extremity of the tailbud (blastema). Secondary structures (neural tube, notochord, somites) arise directly from mesenchyme without germ layers as an intermediate. Whole arrows denote the progress of development.

As seen in Handrigan, 2003

On the other hand, a growing body of literature support the existence of a stem cell population resident in the vertebrate tailbud. The idea that the posterior end of the vertebrate embryo consists of an uncommitted group of cells was recently strengthened by two separate studies. The earliest study has shown in mouse the existence of a unique and permanent pool of bipotential stem cells within the tailbud that can give rise to both neural and mesodermal derivatives all along the axis using retrospective clonal analysis (RCA) with a ubiquitous promoter (Tzouanacou *et al*., 2009; Nicolas *et al*., 1996). This cell fate decision between the neural and the mesodermal cell lineages is continuously made within the tailbud until the late developmental stages during tailbud outgrowth. The second suggested the existence of a stem cell zone in zebrafish through a combination of genetic manipulation of the *Wnt* signalling pathway and single cell

transplantation techniques (Martin and Kimelman, 2012). However, it is important to bear in mind that this study only provides indirect evidence regarding cell fate decision, since the behaviour of the transplanted cells in a genetically-modified environment might not accurately reflect what these cells do in their normal environment. Thus, this longstanding controversy over the potency of tailbud cells in anamniotes remains unanswered.

I.4. Posterior body elongation – Growth vs. tissue deformation

One can imagine that posterior body elongation can be achieved either by anisotropic growth (proposed by Holmdahl's blastemal model), tissue deformation (proposed by Pasteels' continuity of gastrulation model), or a combination of both. Tissue elongation driven by anisotropic growth must ultimately require either an increase in number or size of cells along the axis of growth. This can be achieved by localized proliferation, oriented divisions or cell elongation. We can take the elongation of the vertebrate long bones as an example of tissue elongation resulting from localized cell proliferation (Wolpert, 2010) (Fig.4A). In an elegant study recently published, Cooper *et al.* (2013) also showed that differential growth rates of the metatarsal chondrocytes (increase of up to 40 times their original volume in the jerboa) are responsible for the differences in feet size between the lesser Egyptian jerboa (*Jaculus jaculus*) and the mouse. As seen during axis elongation in zebrafish (Gong *et al.*, 2004) (Fig.4B), tissue elongation can also be achieved by oriented cell divisions, with cell divisions aligned along the axis of growth. On the other hand, tissue elongation driven by tissue deformation may be achieved

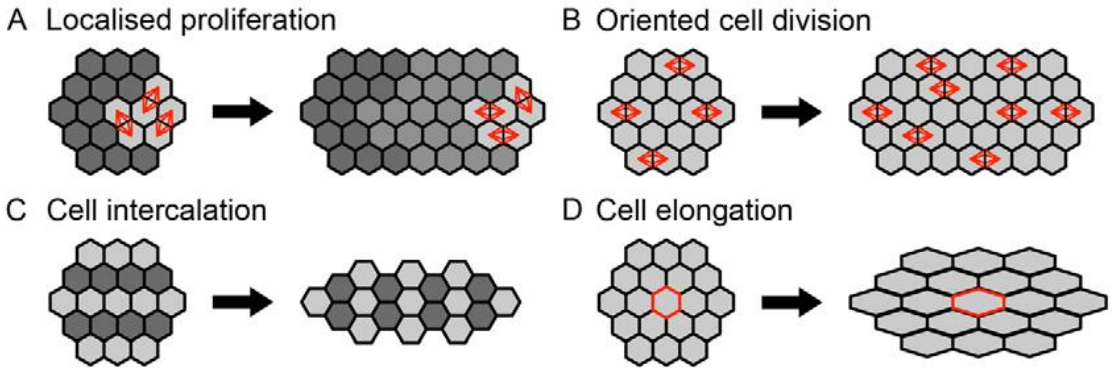

Figure 4. Cellular mechanisms of tissue elongation. Localized cell proliferation **(A)**, alignment of cell divisions **(B)**, cell rearrangements **(C)** and changes in cell shape **(D)** can lead to tissue elongation.
As seen in Economou *et al.*, 2013

through: (1) cell rearrangements as seen in the cell intercalation movements during convergent extension of the vertebrate body axis (Keller, 2006) (Fig.4C); and (2) cell shape change that is known to play a role during germ band elongation in *Drosophila* for instance (Blanchard *et al.*, 2009) (Fig.4D).

I.5. Morphometric analysis of the zebrafish tailbud

The relative contribution of anisotropic growth *vs.* tissue deformation to the process of posterior body elongation is as yet unknown. With the advent of tools for imaging, such as confocal imaging, and the gradual improvement of image analysis software, we can now perform 3D reconstructions of a structure of interest and precisely measure the volume and shape (length, height and width) of the given structure. This type of approach, called a morphometric approach, facilitates the analysis of quantitative variation, generally involves determining the volume and measuring the shape of a tissue, and is most useful for the study of a process throughout the development of a given structure (Roth and Mercer, 2010).

Morphometric analysis of embryonic shape and organ rudiments has already been performed during gastrulation in live and fixed zebrafish embryos (Sepich et al., 2005). These methods allowed not only to quantitatively assess the movements of cell populations *in vivo*, but also to determine whether cell fate and/or movements are disturbed. Although extensively used in the last years for several applications, there has not been any study taking advantage of morphometric analysis methods to investigate the contribution of anisotropic growth and tissue deformation to the shaping of the zebrafish posterior body. In this context, we decided to take advantage of the Imaris software to determine the dimensions of the posterior segments during tailbud outgrowth in zebrafish embryos ranging from 14 up to 25,4 *hpf*.

I.6. Retrospective clonal analysis (RCA)

In an effort to investigate whether the progenitor pools within the zebrafish tailbud display a proliferative/dispersal or stem cell-like mode of growth we have taken advantage of a genetic approach to lineage analysis called retrospective clonal analysis (RCA). RCA is based on the random and heritable labelling of single cells, allowing the retrospective analysis of all their clonal descendants on a long-term basis (Petit *et al.*,

2005). The temporally inducible RCA method we established in zebrafish is based on the ubi:cre^{ERt2}/ubi:Switch system (Mosimann *et al.*, 2011). This tool involves a 4-OHT inducible, CRE-mediated heritable expression of a mCherry reporter. It is also known that the reporter construct has an ubiquitous expression throughout zebrafish development. The use of an inducible system allows for an estimation of the time at which the progenitor cells were labelled. Several requirements must be met to ensure that labelling events correspond to clones that reflect the full range of cell behaviours at play. Firstly, the reporter must be able to be expressed in all cell types of the structure of interest. However, only after the production of an exhaustive library of clones (with a clone being defined as the entire progeny of a particular single cell) will we know whether any cell can be labelled under clonal conditions. Secondly, the frequency of labelling events must vary in response to the modulation of the parameters of the inducing system. Thirdly, the frequency of labelling events must be able to be reduced to a level lower than 10%, corresponding to an extremely low likelihood (less than 1%) for the occurrence of a multiple labelling event per embryo. Fourthly, there must be little or no activity of the reporter in the absence of induction. Most of the validation of our temporally inducible RCA method was conducted during my M1 internship but I continued to test different parameters during my M2 internship.

Regardless of the labeling system selected, unlike classical fate mapping, RCA is unbiased, large-scale and exhaustive as it can label any cell. This allows for visualization of rare events, such as stem-like behaviours as well as the precursor pool mode of growth (proliferative/dispersal or stem-like). A self-renewal mode of growth with stem cells located in the tailbud would be expected to produce long clones that are anchored in the tail. Furthermore, asymmetry regarding the cell fate of the progeny would be indicative of a stem-like mode of growth. In contrast, a proliferative/dispersal mode of growth would generate a series of clones distributed along the axis of growth without anchorage in the tail and with variable lengths.

Drawing from the topographical characteristics of the clones (cell number per clone, clone antero-posterior position and extension, cell fates, frequency of each clonal category), retrospective clonal analysis should provide insights into the growth modes, size, number and location of the precursor pools within the tailbud.

II. Objectives

Although the different phases leading to zebrafish tailbud formation have been extensively characterized, the mechanisms underlying this process continue to generate controversy as of today. Throughout the years, two prevailing models have been proposed to explain posterior body elongation: one defending that this process is driven by a highly proliferative and not fate-restricted posterior growth zone and another arguing that tissue rearrangements of fate-restricted progenitors, similar to those observed during gastrulation, are the key factors at play. We hypothesize that rather than being driven solely by one of these mechanisms, tailbud outgrowth results from the combination of growth from a group of tailbud-resident cells together with dynamic cell behaviours, such as oriented cell divisions, rearrangements and changes in cell size and shape. Thus, in an effort to analyse these processes at the tissue level and determine the relative contribution of these two mechanisms for zebrafish tailbud outgrowth we have performed a series of experiments, including morphometric analysis and RCA devised to assess:

- **i.** Dimension (*i.e*. length, width, height and volume) of posterior segments
- **ii.** Tailbud cell division patterns
- **iii.** Clone characteristics (frequency, identity and distribution) at the tailbud level

Assessing the volume and shape of the structure over time will show the relative contribution of growth and tissue deformation to the posterior body elongation, whereas analysis of specific cell behaviours will tell us how growth and/or tissue deformation are achieved.

III. Materials and Methods

III.1. ubi:cre^{ERt2}/ubi:Switch System (lines II, V and Switch)

In our study we used three different transgenic lines: one harbouring the reporter construct [Tg(-3.5ubi:loxP-EGFP-loxP-mCherry) or (ubi:Switch); Mosimann *et al*., 2011] and two harbouring the inducer construct [Tg(-3.5ubi:cre^{ERt2};cmlc2-EGFP) or (ubi:cre^{ERt2}) line II and line V; Mosimann *et al*., 2011] (see Fig.5A). ubi:cre^{ERt2} line V is known to present a stronger Cre^{ERt2} activity than line II. Driven by the ubiquitin promoter, both the reporter and the inducer are ubiquitously expressed. ubi:Switch carriers can be identified through the ubiquitous EGFP expression. In ubi:cre^{ERt2} lines, EGFP expression is under the control of a cardiomyocyte-specific promoter (cmlc2:EGFP). Hence, ubi:cre^{ERt2} carriers can be identified by their strong EGFP expression in the heart (see Fig.5B, top panel). In double heterozygous transgenic embryos (ubi:cre^{ERt2};ubi:Switch) treated with 4-OHT, cytoplasmic Cre^{ERt2} binds to the 4-OHT and is subsequently translocated to the nucleus where it promotes the conversion from EGFP to mCherry expression (see Fig.5B, bottom panel). Only the ubi:Switch carriers were analysed for the presence of mCherry expression under a Leica MZ16-F fluorescence stereomicroscope. Because of the heterozygous state of both parental lines, only half of the ubi:Switch carriers are expected to be double heterozygous. The

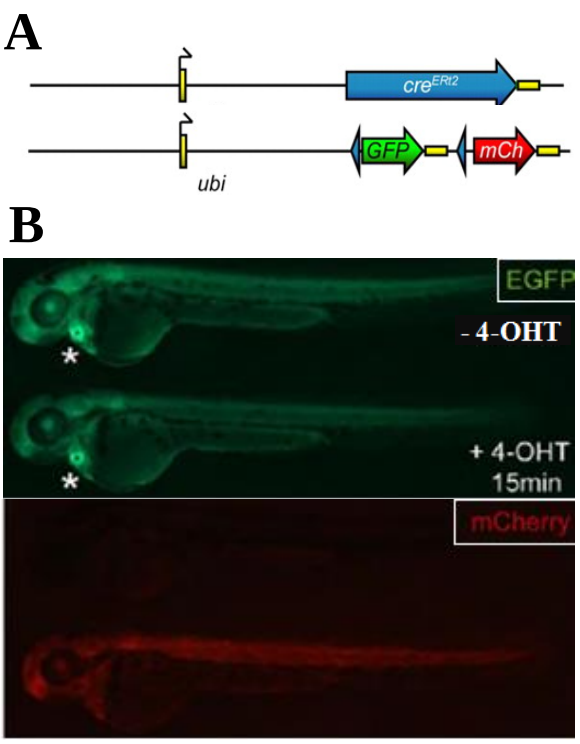

Figure 5. The ubi:cre^{ERt2}/ubi:Switch system. (A) Schematic figure of the ubi:Cre^{ERT2} transgene and the ubi:loxP-GFP-loxP-mCherry reporter cross. **(B)** Live imaging of ubi:creERt2/ubi:Switch double positive zebrafish embryos at approximately 3 days post-fertilization for baseline GFP expression **(top panel)** and mCherry indicating successful loxP excision **(bottom panel)**. On both panels the -4-OHT controls are shown on the top, whereas the embryos treated with 4-OHT are shown on the bottom.
Adaptaded from Mosimann *et al*., 2011

frequency of mCherry labelled embryos was calculated by dividing the number of labelled embryos by the expected number of double heterozygous.

III.2. 4-OHT treatment for Cre^{ERt2} induction

4-Hydroxytamoxifen or 4-OHT (SIGMA cat#H7904) is lipid-soluble and thus can penetrate through cell membranes and the chorion. 4-OHT is light- and temperature-sensitive. A 10 mM working stock solution in ethanol was kept in single-use aliquots at -20 ºC in the dark. The entire clutches obtained from the crosses between one ubi:cre^{ERt2} line and the ubi:Switch line was used and split in multi-well dishes for 4-OHT induction at different concentrations or as controls (no 4-OHT-treatment). Prior to induction, up to 50 collected embryos of the same developmental stage were kept in a single well of a six-well plate with fresh embryo medium. Afterwards, we phenotypically characterized each adult fish in order to use the same couples in each experiment. Also, each clutch was analysed individually in order to track its parental origin. The prepared induction solution was kept in the dark (covered by aluminium foil). In order to induce Cre activity in cre^{ERt2}-expressing embryos, all medium was removed and replaced with 5 mL of embryo medium freshly mixed with 4-OHT. The 4-OHT concentration used and the induction stage vary between experimental procedures. Immediately after, the treated embryos were placed into a 28 ºC incubator in the dark, to allow for efficient induction. The induction solution was removed after 5 or 15 minutes, depending on the experimental procedure, and the embryos were thoroughly rinsed once, followed by three 5-minute washes under agitation and two more rinses, to remove all traces of 4-OHT. The embryos were subsequently placed in a petri dish containing fresh embryo medium and grown at 28 ºC. The next day we changed the medium for embryo medium with 0.003% Propylthiouracil (PTU), which inhibits the formation of pigments. For the 10 µM induction experiment, we replaced the induction solution daily to maintain Cre^{ERt2} activity.

III.3. Analysis of the clone characteristics and confocal imaging

Clone characteristics (frequency, number of cells labelled, their position along the anterior-posterior axis and cell identity) were screened three days after performing the 4-OHT-mediated Cre^{ERt2} induction, under a Leica MZ16-F fluorescence

stereomicroscope. Preliminary screenings at one day post-induction (dpi) revealed a very faint expression of mCherry, almost imperceptible. The time required for the translocation of the cytoplasmic Cre^{ERt2} to the nucleus, recombination of the loxP sites, mRNA transcription of the mCherry reporter and subsequent protein translation and folding, may lead to the insufficient accumulation of mCherry after 1 day. We thus decided to perform the screening at 3 dpi to enable mCherry sufficient accumulation over the detection threshold.

To record the clones, embryos were imaged in a lateral view using a Leica SP-5 confocal microscope with a 10x or 40x objective. Confocal z-stacks through the entire embryo posterior body were acquired with a 2 µm z-step. Embryos were anesthetized with tricaine (0.16 mg/ml) and embedded in 5% methylcellulose. Since this is an inverted microscope, the embryos were placed in a bottom glass dish. Embryos were then fixed in PFA 4% and stored for future analysis.

III.4. Confocal imaging of fixed embryos and morphometric analysis

For our morphometric analysis we labelled the membrane and the nucleus with fluorescent markers by co-injecting 1 nl of a mix of nuclear mCherry (0.35 µg/µl) and membrane GFP mRNAs (0.4 µg/µl) at the one-cell stage in order to achieve ubiquitous labelling. From the injected clutches of embryos, we collected the brightest embryos. At the appropriate stage (from 14 up to 25,4 *hpf*), injected embryos were anesthetized in embryo medium with tricaine (0.16 mg/ml), fixed in 4% PFA and embedded in 1% low-melting-point agarose in glass bottom dishes. Embryos were oriented in a lateral position. This is the position in which the thickness of the tissue is the lowest, allowing better imaging. Laser scanning confocal data was acquired using a Leica SP-5 confocal microscope. Fluorophores were excited using a 488 nm argon laser (GFP) and a 514 nm DPSS laser (mCherry). We used a 10x objective to capture the entire posterior body region. Confocal images were acquired as z stacks of xy images taken with a 2 µm Z-step size. The channels were acquired simultaneously and imported into ImageJ, where channels were split. Uniform contrast and brightness adjustments were made using Adobe Photoshop.

Our laser scanning concofal data on fixed ubiquitously labelled samples was then processed and surface reconstructions of all the posterior segments, pre-somitic mesoderm (PSM) and tailbud (TB) of embryos ranging from 10 up to 32-somites (14 up

to 25,4 *hpf*) were done with the combination of the MeasurementsPro and surface functions of the Imaris software (Bitplane AG). This was done by manually contouring the feature of interest within the region of interest at regular z-intervals. We then determined the dimensions (*i.e.* length, width, height and volume) of the entire posterior body from the dimensions of all the resulting surface renderings (*i.e.* from the dimensions of all the segments). Furthermore, both the length and volume of the entire posterior body were calculated by summing the lengths of all the segments, whereas both the width and height were calculated by averaging over all the segments.

In order to analyse the variation of each of these parameters throughout tailbud elongation, we plotted the mean values obtained from several measurements at each developmental stage against time (displayed in *hpf*) accompanied by the corresponding standard deviation bars. Afterwards, we also calculated the elongation rate (*ER*) and fold increase (*FI*) for each of these parameters during the two phases of posterior body elongation we identified from our first observations – phase 1 (ranging from 14 *hpf* up to 21 *hpf*) and phase 2 (from 21 *hpf* up to 25,4 *hpf*) – using the expressions:

$$ER_{Phase1} = \frac{x_{21hpf} - x_{14hpf}}{21hpf - 14hpf}$$

$$ER_{Phase2} = \frac{x_{25,4hpf} - x_{21hpf}}{25,4hpf - 21hpf}$$

$$FI_{Phase1} = \frac{x_{21hpf}}{x_{hpf}} \qquad FI_{Phase2} = \frac{x_{25,4hpf}}{x_{21hpf}}$$

, where *x* represents the mean values (n= 3 embryos) obtained at the extreme time points of each phase for a given parameter.

III.5. Cecyil fish

In order to analyse the zebrafish tailbud mode of growth, we monitored tailbud outgrowth in embryos belonging to a transgenic fish line called Cecyil (*ce*ll *cy*cle *il*luminated), harbouring a set of cell cycle markers coupled with different fluorescent molecules that enable the detection of cells undergoing S/M/G2 (green) or G1 (red) phases (Sugiyama *et al*., 2009). To analyse the pattern and distribution of labelled cells, embryos were then imaged under a Leica SP-5 confocal microscope following the parameters described below.

III.6. Image acquisition of fixed Cecyil embryos

Laser scanning confocal data was acquired using a Leica SP-5 confocal microscope. Fluorophores were excited using a 488 nm argon laser (GFP) and a 561 nm DPSS laser (DsRed). Embryos were anesthetized with tricaine (0.16 mg/ml), fixed in 4% PFA and embedded in 1% low-melting-point agarose in glass bottom dishes. Embryos were oriented in a lateral position. We used a 10x objective to capture the entire posterior body region. Confocal images were acquired as z stacks of xy images taken with a 2 μm Z-step size. These imaging parameters were selected in order to ensure the viability of the embryo while maintaining enough image resolution for automated analysis. The channels were acquired simultaneously and imported into ImageJ, where channels were split. Uniform contrast and brightness adjustments were made using Adobe Photoshop.

IV. Results

IV.1. Tailbud elongation undergoes two distinct phases

As a starting point, we decided to investigate in more detail the mechanism(s) responsible for posterior body elongation by monitoring zebrafish tailbud outgrowth using large-scale 4-D morphometric analysis. We defined segments as the portion of posterior body that corresponds to two consecutive somites: segment 13-14 is the portion of the body at the level of somites 13 and 14; the unsegmented region and the tailbud are each a segment. To this end, the length, width, height and volume of posterior segments (*i.e.*, the segments that will give rise to the posterior body, that in zebrafish correspond to segment 13-14 up to the most caudal segment, the tailbud) of embryos from 10 (14*hpf*) up to 32 somites (25,4*hpf*) were determined using the Imaris software, as shown in Fig.6A–C and Fig.7A–C. As expected, we observe that the embryo length increases over time from the earliest 10-somite stage up to the latest 32-somite stage (Fi g.6D). However, it is worth noting that this increase in embryo length is not constant and can be subdivided into two distinct phases: the first phase ranging from

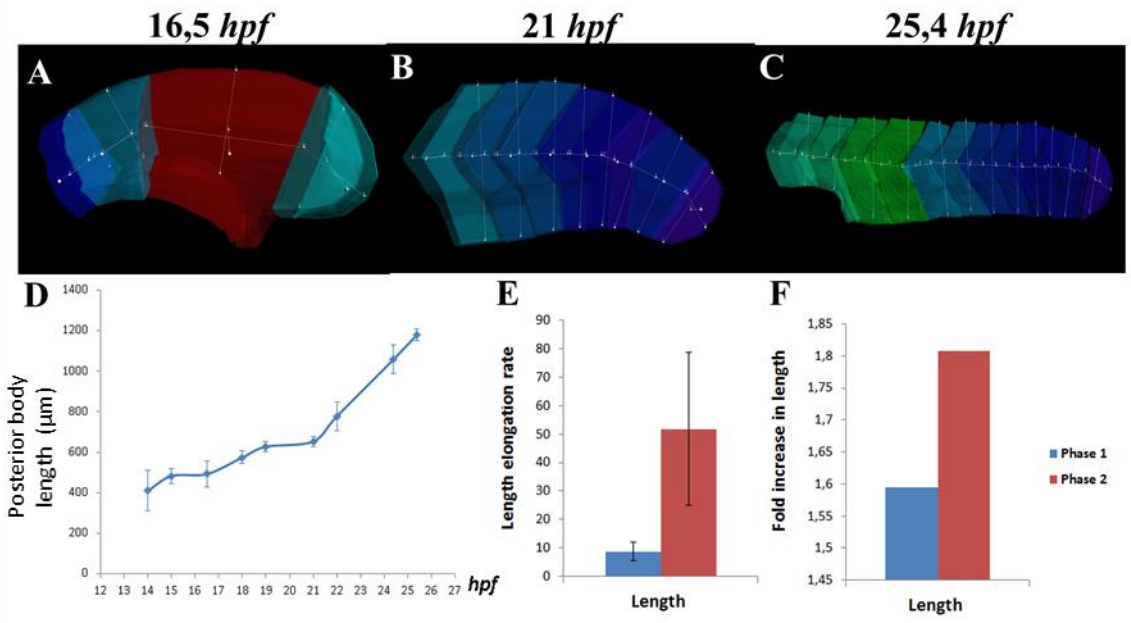

Figure 6. Tailbud elongation undergoes two distinct phases. Embryo length was assessed using the Imaris software in embryos from 14 up to 25,4*hpf.* The length measurements (yellow line) performed on embryos at 16,5, 21 and 25,4 *hpf* are exemplified in panels **(A)**, **(B)** and **(C)**, respectively. The posterior body length is plotted against time in **(D)**. The quantification of the elongation rate and fold increase in length are shown in **(E)** and **(F)** respectively, where phase 1 is shown in blue and phase 2 in red.

14 up to 21*hpf* (*i.e.*, from 10 up to 24 somites) when the embryo length increases slowly over time and the second phase taking place from 21*hpf* onward, when the embryo length increases more rapidly (Fig.6D). To describe further these two phases, we quantified the speed and amount of length increment during phase 1 and phase 2 by calculating the elongation rate and fold increase in elongation in both phases. Our results clearly show that during phase 2, both the elongation rate and the fold increase are significantly higher (Fig.6E, F) than in phase 1. The posterior body therefore elongates more and faster during phase 2. Tailbud elongation in zebrafish clearly undergoes two distinct phases.

IV.2. Tailbud outgrowth relies both in tissue deformation and growth

We next decided to investigate whether we could detect significant changes in tissue shape by directly analyzing the width and height of the posterior body over time. Our results demonstrate that during phase 1, the posterior body width tends to decrease over time, whereas the height has a tendency to increase (Fig.7D), supporting the idea that

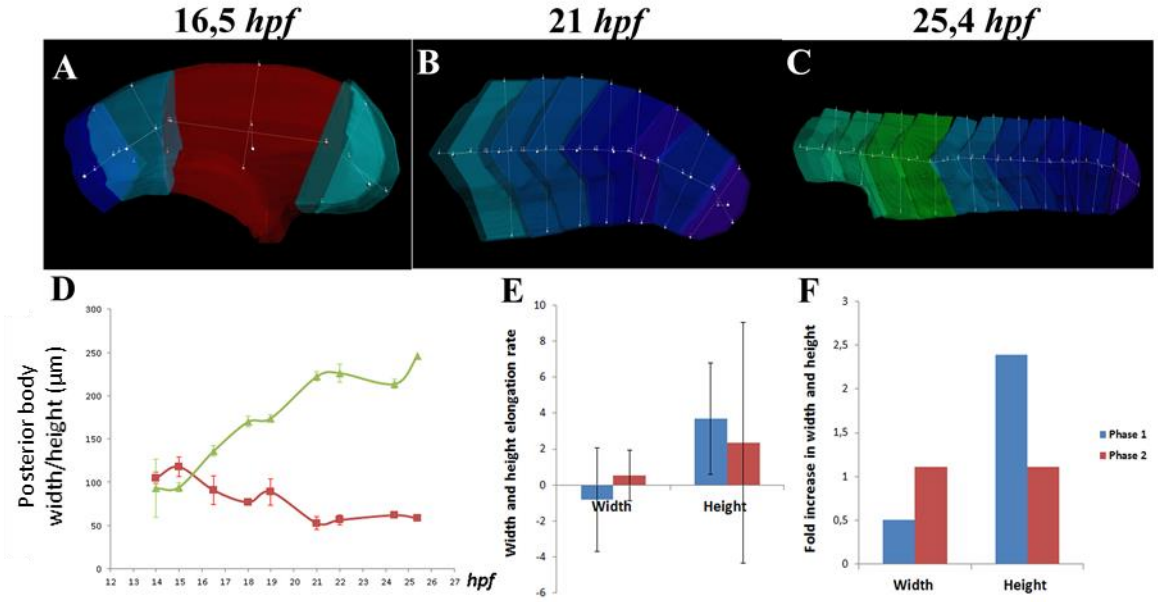

Figure 7. Tailbud elongation relies on alterations in posterior body shape. Posterior body width and height were assessed using the Imaris software on embryos from 14 up to 25,4*hpf*. The width (red line) and height (yellow line) measurements performed on embryos with 16,5, 21 and 25,4*hpf* are exemplified in panels **(A)**, **(B)** and **(C)**, respectively. The posterior body width (red curve) and height (green curve) are plotted against time in **(D)**. The rate of width and height variation during the first phase (in blue) and the second phase (in red) are shown in **(E)**. The fold increase in width and height are shown in **(F),** with phase 1 in blue and phase 2 in red.

significant changes in tissue shape are taking place. More precisely, the structure is getting thinner, taller and longer. However, this scenario is completely different during the second phase, where both width and height seem to have reached a *plateau* (Fig.7D), suggesting that changes in tissue shape during this phase are much more subtle. This difference between phase 1 and 2 is confirmed when we compare the rates and fold increase of width and height variations. Regarding the width, both the rate and fold increase are negative during the first phase and almost null in the second phase, which is consistent with the decrease and subsequent stabilization observed during phase 1 and 2, respectively (Fig.7E, F). Similarly for the height, both the rate and fold increase are higher during phase 1, thus supporting the previous results showing an increase during phase 1 and a stabilization in phase 2 (Fig.7E, F).

Next, we wished to investigate whether growth could play an important role during tailbud elongation by measuring the volume of posterior body and evaluating its variation over time. Our results indicate that, the variation of posterior body volume also exhibits two phases: it is stable during phase 1 and increases during phase 2 (Fig. 8A). This is corroborated by the volume variation rate and the fold increase in volume that are both null in phase 1 and high in phase 2 (Fig. 8B–C). These observations indicate that growth is a major contributor to tailbud elongation during the second phase of posterior body formation.

Taken together, these results suggest a scenario where different processes act at different time-points in order to drive tailbud elongation: whereas during phase 1, the slow increase in embryo length at constant volume accompanied by a decrease in width and an increase height suggest that tissue deformations are the principle cause of

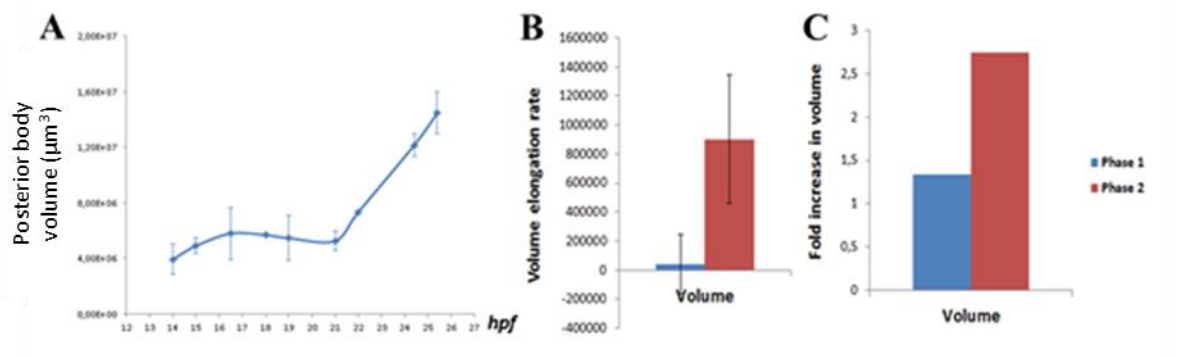

Figure 8. Tailbud elongation relies on growth. The posterior body volume is plotted against time in **(A)** and the rate of volume variation during the first phase (in blue) and the second phase (in red) is shown in **(B).**The fold increase in volume is shown in **(C)**, with phase 1 in blue and phase 2 in red.

elongation during this first phase, the rapid increase in length and volume together with width and height stabilization indicate minor changes in tissue shape but a major role for an accentuated growth during phase 2.

IV.3. Myogenesis and notochord inflation correlate with growth in early born segments

Although our previous results highlight the importance of growth especially during the second phase of tailbud elongation, the antero-posterior levels where the posterior segments undergo these physical modifications within the 21-25,4*hpf* time frame remain to be identified. Thus, we analyzed the volume variation over time displayed by each

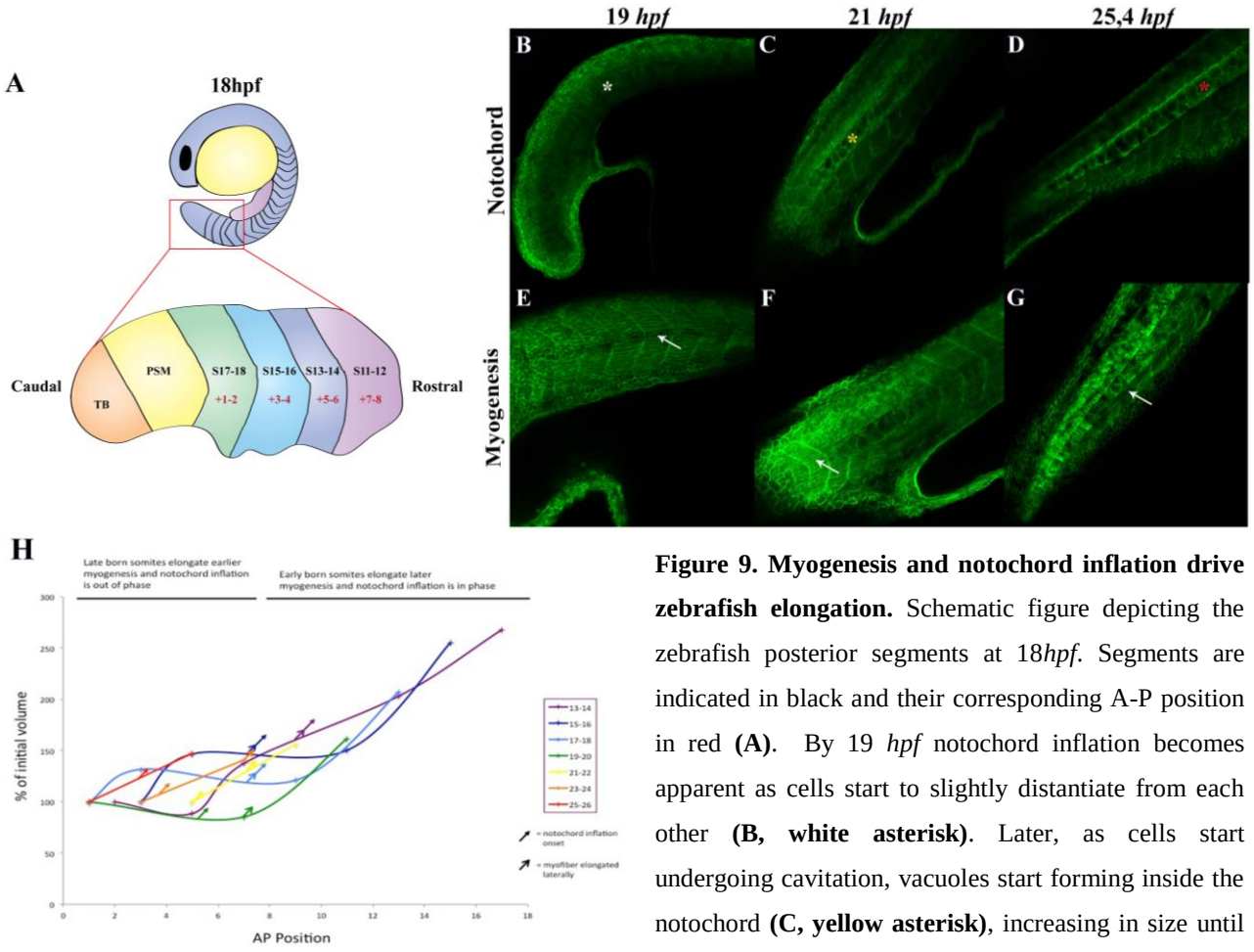

Figure 9. Myogenesis and notochord inflation drive zebrafish elongation. Schematic figure depicting the zebrafish posterior segments at 18*hpf*. Segments are indicated in black and their corresponding A-P position in red **(A)**. By 19 *hpf* notochord inflation becomes apparent as cells start to slightly distantiate from each other **(B, white asterisk)**. Later, as cells start undergoing cavitation, vacuoles start forming inside the notochord **(C, yellow asterisk)**, increasing in size until they occupy the whole extension of the notochord **(D, red asterisk)**. The last somite where myofibers are elongated laterally is indicated with a white arrow in panels **(E–G)**, corresponding to somite 12 (19 *hpf*), 17 (21 *hpf*) and 26 (25,4 *hpf*), respectively. Panels **(B-G)** represent maximum intensity projections of z-stacks acquired from PFA(4%)-fixed embryos ubiquitously labelled with membrane-targeted GFP highlighting the cell contours using a Leica SP5 confocal microscope. The volume of each posterior segment is plotted against its position on the A-P axis in **(H)**.

posterior segment, using embryos from 10 (14*hpf*) up to 30 somites (24,4*hpf*). To be able to register and thus compare the evolution of each posterior segment, the volume of each segment was plotted against its position on the antero-posterior (A-P) axis, position +1-2 corresponding to the last segment formed (Fig. 9A). For example, in a 18-somite stage embryo, the position +1-2 corresponds to segment 17-18. By doing so, we observed that from position +7-8 up to position 17-18 in embryos ranging from 21 up to 24,4*hpf*, the increase in volume becomes much more accentuated (Fig.9H), suggesting that growth is taking place mainly in the early born segments, that include the first three posterior segments forming in the embryo (*i.e.*, segment 13-14, segment 15-16 and segment 17-18).

After determining that early born segments correspond to the posterior segments displaying major growth during posterior body elongation, we were interested in investigating which biological processes could correlate with this tissue response. Upon carefully monitoring these embryos throughout tailbud outgrowth, we discovered two possible mechanisms that were good candidates to explain our previous observations. The first is a phenomenon known as notochord inflation, a process in which notochord cells undergo cavitation, becoming highly enlarged in volume in a rostral-to-caudal fashion (Fig.9B–D). The second is myofiber maturation during which a subset of muscle cells start to fuse with each other, forming long myotubes, after that another subset of muscle cells have elongated and relocated to the somite surface (Fig.9E–G). These behaviors result in alterations in somite shape and size. In order to investigate whether these processes correlate with growth, we observed and annotated for each embryo stage the segment corresponding to the posterior-most segment where notochord inflation could be observed, as well as the posterior-most segment where elongated myofibers were located laterally in the somites. Afterwards, we compared these observations with the variation in volume displayed by all the posterior segments. By doing so we were able to conclude that the increment in volume observed from position 7-8 up to position 17-18 in embryos ranging from 21 up to 24,4 *hpf* is coincident with the onset of notochord inflation and myofiber maturation in these stages, indicating that both processes seem to be directly involved in posterior body growth (Fig.9H). Furthermore, we also observed that in early born segments, notochord inflation and myofiber maturation are initiated when these segments occupy a more anterior position compared to that of late born segments. In addition, in early born

segments, the onset of notochord inflation and myofiber maturation occur simultaneously while in late born segments, the onset of notochord inflation and myofiber maturation are slightly out of phase (Fig.9H). Together, these observations indicate that both processes of notochord inflation and myofiber maturation progress posteriorly faster than segment formation, with notochord inflation progressing slightly faster than myofiber maturation.

IV.4. Lack of persistent proliferation in the zebrafish tailbud suggests the absence of a pool of resident stem-cells

In order to shed some light into the zebrafish tailbud mode of growth either proliferative/dispersal or stem-like, we monitored tailbud outgrowth in embryos belonging to a transgenic fish line called Cecyil, harbouring a set of cell cycle markers coupled with different fluorescent molecules that enable the detection of cells undergoing S/M/G2 (green) or G1 (red) phases (Sugiyama *et al*., 2009). Our results

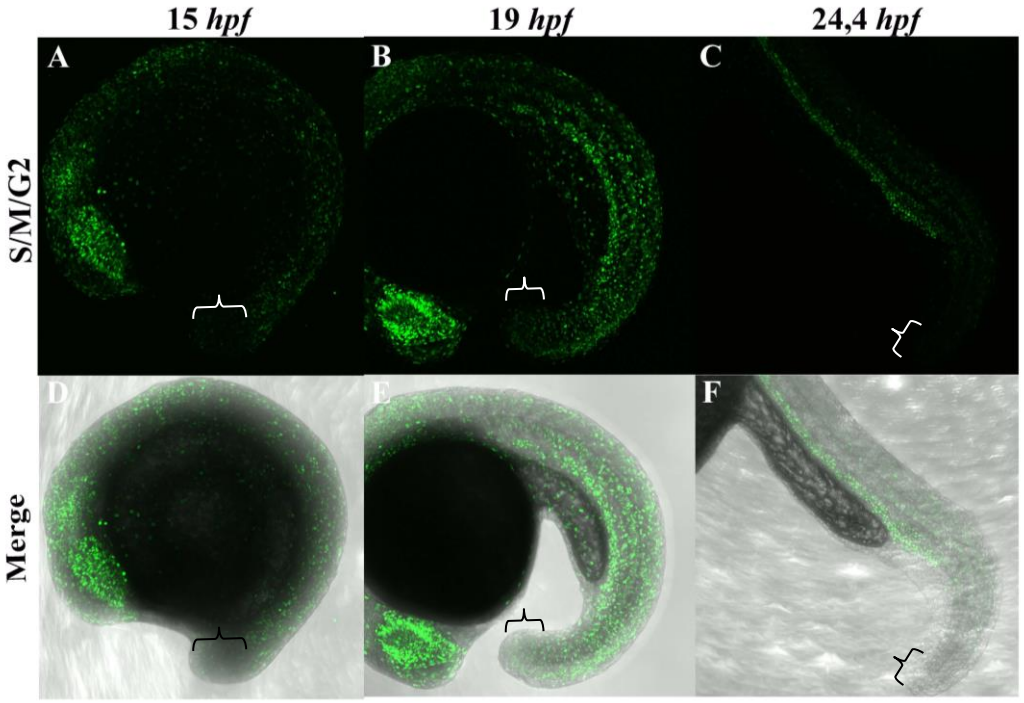

Figure 10. The zebrafish tailbud does not contain a pool of resident proliferative progenitors. Representative maximum intensity projection of PFA-fixed Cecyil embryos during posterior body formation, visualizing proliferating cells (green; **A-C**). Developmental stages are expressed in *hpf*. Z-stacks were acquired from live embryos using a Leica SP5 confocal microscope equipped with an objective lens (x10 N.A. 0.3). Panels **(D-F)** represent a single bright field plane merged with the green signal to better visualize the embryonic structures. Brackets delimit the tailbud region.

demonstrate that whereas at the earliest developmental stages (from 12 to 15*hpf*), the green signal predominates indicating that cells are undergoing rapid mitotic cycles (Fig.10A and D), as the embryo grows, the colour balance is reversed (Fig.S1). At later stages the green signal becomes restricted to specific tissues (*e.g.* retina) (Fig.10B and E), whereas the red signal highlights well-differentiated cells (*e.g.* muscle cells) (Fig.S1). Focusing our attention on the tailbud region, we were not able to detect a persistent and strong green signal that could be indicative of the presence of a tailbud-resident long-term proliferative progenitor pools (Fig.10). This observation shows that after an early phase of intense proliferation, little to no proliferation occurs in the tail bud at late stages. Although we cannot rule out the existence of a small pool of resident stem cells with a slow division rate, this suggests that unlike mouse, zebrafish tailbud outgrowth does not rely on a stem-like mode of growth but rather on a proliferative/dispersal mode of growth at the early stage.

IV.5. Our RCA preliminary results are consistent with a proliferation/dispersion - like mode of growth

In order to confirm these results, we concentrated our efforts on the development of a temporally inducible retrospective clonal analysis ideally suited for the zebrafish embryo that would enable us to examine the lineage history of all the posterior body precursors and thus further elucidate the zebrafish tailbud mode of growth either proliferative or stem-like. Starting during my M1 internship, we tested two transgenic lines that express ubiquitous tamoxifen-inducible Cre recombinase, that were combined with a ubiquitous reporter line, the ubi:Switch (see Materials and Methods for details).

As a starting point, we had to make sure our system complied with a set of conditions necessary for validating our observations. First, as it had been previously noted that inducible Cre systems can be leaky, resulting in constitutive rather than inducible activation (Petit *et al*., 2005), we decided to examine the leakiness of our system by testing whether labelling could be induced in the absence of 4-OHT. Our preliminary results demonstrated that untreated control embryos did not exhibit mCherry expression, suggesting that if there were leaks in the system their frequency was much lower compared to the clones (less than 1%), thus validating our system for further studies. Second, we had to make sure our reporter could be ubiquitously expressed upon induction, allowing the labelling and subsequently tracing of all the posterior body

precursors. In order to test this, we crossed the ubi:cre^{ERt2} lines (line II or line V) with ubi:Switch line and submitted the embryos to a continuous high concentration of 4-OHT (10 μM; as described in Methods) to achieve high Cre^{ERt2} responses. By doing so, we were able to detect widespread labelling, in the sense that it encompassed a large fraction of the cells broadly scattered all along the body axis, including neural tube, notochord, gut, surface ectoderm, fin and muscle cells. With this result we confirmed that the reporter can be expressed in most if not all tissue types in the posterior body, indicating that our system is suited for tailbud lineage tracing experiments.

After verifying that our system met the requirements necessary to establish a temporally inducible retrospective clonal analysis strategy, we had to determine a set of right parameters that would enable us to modulate induction in such a way that we would be able to conduct our experiments under clonal conditions, *i.e.*, when the frequency of embryos labelled is lower that 10%. First, we had to select which embryonic stage would be more suitable to perform the inductions. Since we wanted recombination to happen prior to the tailbud outgrowth, which in zebrafish starts at about 10*hpf*, we

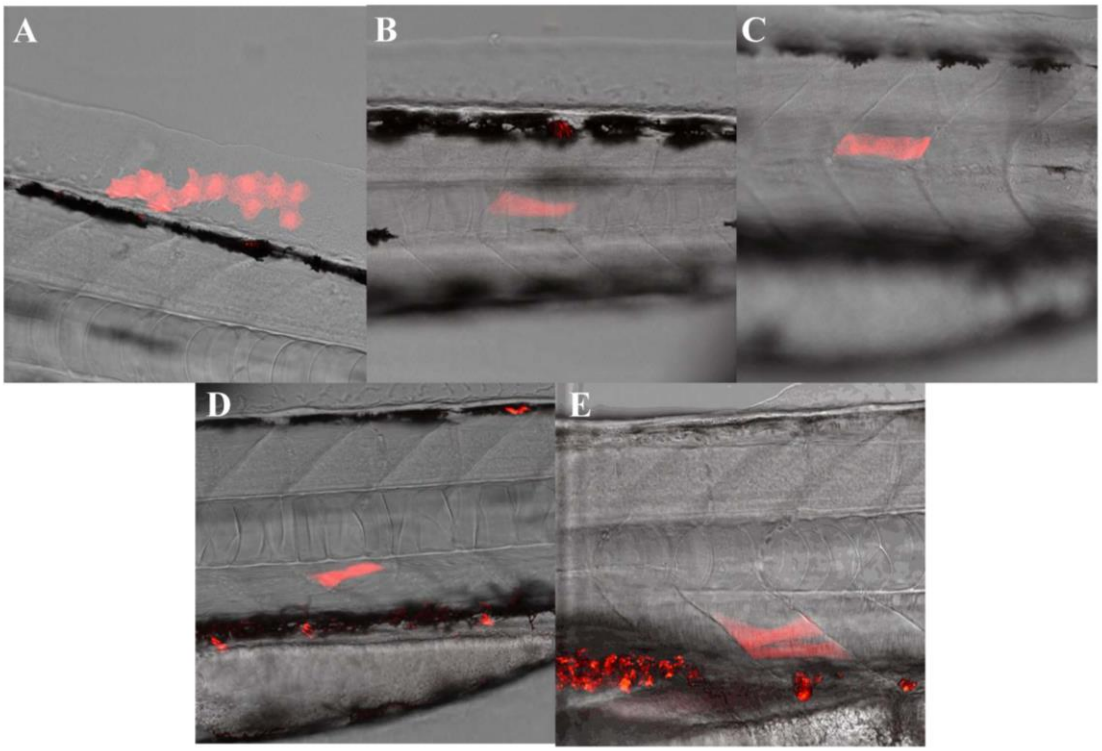

Figure 11. Clones obtained by temporally inducible retrospective clonal analysis. The small library of clones is exemplified in panels **(A)** to **(E)** where we can observe labelling in surface ectoderm cells at the level of somite 23 **(A)** and in muscle fibers located on somite 19, 12, 10 and 5 **(B– E)**, respectively. These clones were obtained from both ubi:cre^{ERt2} lines II and V, induced at 4 *hpf* with 15 nM of 4-OHT for 5 min.

decided to perform inductions at 4*hpf* (sphere stage) and 8*hpf* (75%-epiboly). The results obtained were similar for both stages, suggesting that the induction time point does not significantly affect the successful recombination.

We then had to play with various parameters that might directly affect the frequency of labelling events, such as different concentrations of 4-OHT, variations of the induction length and different ubi:cre^{ERt2} lines, in order to reach optimal clonal conditions. After performing several tests, we observed that whereas the first two parameters affected the frequency of labelling events in a concentration/time-dependent manner, the latter did not seem to have a significant effect on labelling extent nor distribution.

Clonal frequencies were reached with 15 nM of 4-OHT and also with 25 nM (Fig.11). From these experiments conducted for a two-year period we were able to generate a small library of 23 clones from both ubi:cre^{ERt2} lines II and V, induced at 4 or 8*hpf* using 15 or 25 nM 4-OHT for 5 min (Table 1). The clones altogether are located over the entire anterior-posterior axis and correspond to a wide range of cell types: surface ectoderm cells (Fig.11A), muscle fibers (Fig.11B–E), neurons and fin cells (Table 1). Up to this point we only identified small clustered unipotent clones and no clones indicative of a stem-cell like mode of growth were found. Although a bigger library of clones has to be built in order to conclusively rule out the existence of a tailbud-resident stem cell pool, as of today these results support the idea that tailbud outgrowth in zebrafish relies on a proliferative rather than a stem-cell like mode of growth, which is consistent with our previous results using the Cecyil transgenic fish line.

Table 1. Library of clones obtained by temporally inducible retrospective clonal analysis.

Number of labelled cells	Cell type	AP position	Number of clusters
2	Muscle fiber	?	1
2	Surface ectoderm	Head	1
2	Surface ectoderm	Head	1
2	Muscle fiber	Somite 4/13	1 or 2
4	Surface ectoderm	Somite 22	1
1	Muscle fiber	Somite 10	1
3	Surface ectoderm	Head	1
1	Muscle fiber	Somite 11	1
1	Muscle fiber	Tail	1
2 + 4	Muscle fiber + Fin	Tail	2
?	Neurons	Somite 11	1
2	Surface ectoderm	Head	1
1	Surface ectoderm	Head	1

10	Surface ectoderm	Fin (Somite 23)	1
1	Muscle fiber	Somite 19	1
1	Muscle fiber	Somite 12	1
1	Muscle fiber	Somite 10	1
?	Neuronal cells	Eye	1
?	Neuronal cells	Eye	1
?	Surface ectoderm	Somite 1	1
3	Muscle fiber	Somite 5	1
2	Muscle fiber	Somite 9	1
1 or 2	Muscle fiber	Somite 4	1

V. Discussion

V.1. Posterior body tissue dynamics

In the present work we found evidence supporting the idea that tailbud outgrowth undergoes two distinct phases in which the embryo posterior segments undergo a series of shape and size modifications. In particular, we observed that whereas segment growth, *i.e.* increase in volume, occurs mainly during the second phase of tailbud elongation, the highest amount of segment shape changes, *i.e.* the most significant variations in segment width and height, takes place mainly during the first phase. Taken together our results support what other authors have previously postulated, arguing that tailbud outgrowth relies on the combination of diverse mechanisms (Keller, 2002), rather than on a single process. Although our study already provided precious insights into the dynamics of tissue growth and remodeling during zebrafish posterior body elongation, the precise events taking place at the cellular level that are the microscopic driving forces of these tissue modifications are not yet completely understood. For instance, considering only segment growth, one can imagine at least two distinct events that could lead to an increase in the segment volume observed at the tissue level: one possible explanation would be the accentuated increase in the number of cells along the antero-posterior embryonic axis; on the other hand it could be simply due to alterations in cell shape and size (*e.g.* cell elongation or cell-cell spacing modifications) that can occur in the absence of cell proliferation. Moreover, one should also keep in mind that the increase in the number of cells in the direction of growth rather than relying solely on cell proliferation, can also be attained through a combination of cell movements, rearrangements and oriented cell divisions (Economou *et al*., 2013). Taking into consideration the substantial amount of studies addressing these issues during the last years, it has been becoming clear that in the majority of cases these complex morphogenetic events rely on an intricate combination of all these cellular processes, rather than on one sole main mechanism. A clear example that morphogenesis often involves the combination of different cellular processes is the vertebrate limb bud. Evidence in the mouse limb bud has shown that proliferation cannot solely be accountable for growth, and that both cell shape and oriented cell divisions are important for driving elongation (Boehm *et al.*, 2010). In this context, we believe it is

reasonable to assume that all these processes could be at play during zebrafish tailbud outgrowth and ought to be properly investigated on an individual basis in order to dissect their relative contribution. Thus, we strongly believe that in the future experiments addressing the following points should be performed:

- **i.** Cell behaviours (*e.g.* cell intercalation) should be performed in the developing zebrafish tailbud by tracking and monitoring individual tailbud cells using 4D live imaging;
- **ii.** Cell shape changes should be carried out by analysing cell segmentation profiles in mosaically labelled movies;
- **iii.** Oriented cell divisions should also be quantified by direct annotation from the generated movies.

For this reason, we developed long-term 4D imaging of the growing tailbud of zebrafish, a vertebrate model ideally suited for long-term live imaging. To do so, we had to find the right parameters to time-lapse the entire posterior body elongation, such as z- and time-step, magnification and how to embed the embryos. By right parameters one means those that allow us not to miss any cell division and to have enough resolution to track cells in space and time (average time-step of 2 minutes and z-step of 2µm). We have started addressing the aforementioned points by: (1) manually annotating all cell divisions in the zebrafish tailbud by marking the x,y,z,t position of each hemi-nuclei with the Imaris measurement point tool in mosaically labelled embryos (by injecting 32-cell stage embryos with nuclear mCherry and membrane GFP mRNAs; see Fig. S2); and (2) generating automated cell tracks of all nuclei and manually selecting the ones originating from the tailbud.

Afterwards, we investigated the biological mechanisms that could correlate with the physical alterations we had observed at the tissue level and we discovered two independent processes taking place during tailbud outgrowth – notochord inflation and myogenesis – that proved out to be excellent candidates to support our previous observations. A recent study provided further evidence, at least for the role of myogenesis in tissue elongation (Bouldin *et al.*, 2014). By taking advantage of a transgenic zebrafish line that misexpresses cdc25a, a key controller of mitotic entry, the authors observed that cells abnormally express MyoD, a transcription factor known to play a critical role in zebrafish muscle formation, and remain in an undifferentiated state. As a consequence, they are not capable of contributing to the formation of

myofibers, and thus to contribute significantly to the lengthening of the embryo (note that ectopic expression of Cdc25a results in the shortening of the embryos). However, further investigation is needed in order to not only confirm the importance of these two biological processes, but also to identify other novel mechanisms that may be actively contributing to tailbud elongation.

Collectively, the data presented in this study points towards a scenario in which growth from the tailbud plays little or no role during zebrafish tailbud elongation and occurs mostly anteriorly, based on the fact that:

- **i.** Growth only starts to increase significantly during the second phase of tailbud outgrowth;
- **ii.** The highest increase in volume is mainly observed in anterior segments;
- **iii.** Cell divisions in Cecyil fish are practically inexistent in the tailbud region;
- **iv.** Our RCA experiments do not suggest the existence of a stem cell pool resident in the zebrafish tailbud.

V.2. The role of cell proliferation during tailbud outgrowth

Finally, combining two different experimental strategies, Cecyil fish and RCA, we tried to investigate in more detail the zebrafish tailbud mode of growth in an effort to find an answer to the longstanding question regarding the potency of tailbud cells that has been generating controversy amongst the scientific community for the past years. In both cases we found no evidence supporting the existence of a stem-cell population resident in the zebrafish tailbud, which lead us to believe that in this vertebrate model tailbud outgrowth relies mostly on the proliferation/dispersion of lineage-restricted progenitors. By taking advantage of a novel zebrafish transgenic line that ubiquitously expresses a photoconvertible protein, together with long-term imaging, Bouldin *et al.* 2014 were able to label groups of posterior progenitors and reveal that they enter a prolonged quiescent phase until they begin to differentiate as somitogenesis proceeds, further supporting the proliferative/dispersal mode of growth in the zebrafish tailbud. This is opposed to what has been shown in the mouse model where it was recently demonstrated that a stem cell pool resides within the tailbud, as it is capable of generating both cells in the neural tube and muscle (Tzouanacou *et al.*, 2009). It also challenges current thinking that the zebrafish tailbud, as seen in the mouse, is populated by a bipotential cell pool (Martin and Kimelman, 2012). However, the latter study was

based on the combination of *Wnt* signalling disruption and single cell transplantation techniques, and thus only provide information over the potency of these cells when challenged, rather than providing an accurate representation of the endogenous cells capabilities in the wild-type normal environment. The discrepancies over the fate decision made within the tailbud between zebrafish and the mouse, might derive from differences in the speed of development, one of the key differences between amniotes and anamniotes. Zebrafish embryos need to develop very rapidly, as it needs to escape predators and feed as soon as possible. In contrast, mouse embryonic development occurs *in utero*, hence protected and can therefore be slower. In this context, one might argue that zebrafish tailbud relies on a rapid proliferative/dispersal mode of growth, as opposed to a slow stem cell mode of growth seen in the mouse.

Although this study already provided some clues on the mechanisms involved in zebrafish tailbud elongation, the preliminary results obtained are not sufficient to draw a definite conclusion and exclude stem cells as one of the key players acting to drive tailbud outgrowth. Therefore, other complementary experiments ought to be performed in the future to validate this hypothesis. In this context, one alternative to confirm that the zebrafish tailbud is indeed devoid of stem cells that may play a role during posterior body formation and relies mostly on the proliferation of lineage-restricted progenitors, would be to perform a double immunohistochemistry on fixed embryos at different developmental stages using antibodies against stemness (*e.g.* Oct4 and Sox2) and proliferation markers (*e.g.* Ki67) that have been previously validated in zebrafish (Robles *et al*., 2011) and check whether it would be possible to identify cells resident in the tailbud positive for both markers. If yes, then the stem-cell like mode of growth hypothesis could not be discarded and would have to be reconsidered, but if, on the other hand, it was possible to identify only $Ki67^{+}$ cells, then we would obtain one more observation supporting the idea that tailbud outgrowth is mainly driven by proliferation of unipotent precursors, which is consistent with the preliminary results present in our study. Although the co-expression of both proliferation and stemness markers would be a first evidence pointing towards the existence of a stem-like mode of growth, the definitive proof could only be attained by performing lineage tracing experiments demonstrating cell fate asymmetry and multipontency. Moreover, the relative contribution of cell proliferation towards elongation has already been quantified in a mutant (*emi1*$^{-/-}$ zebrafish mutant), in which the cell cycle is arrested shortly after the

beginning of gastrulation, resulting in a 22% reduction on axis elongation (Zhang *et al.*, 2008). However, an alternative approach using specific DNA replication inhibitors (*e.g.* Aphidicolin and Hydroxyurea) that cause cell cycle arrest at the S phase would also be an interesting trail to pursue since, unlike the *emi1*$^{-/-}$ zebrafish mutant, it would allow to block cell divisions at specific time-points, and thus more precisely evaluate their impact on posterior body formation. During these assays embryos are placed inside a solution containing both DNA replication inhibitors while the control counterparts are placed inside a DMSO solution and incubated until fixation. To assay for DNA synthesis after drug incubation, BrDU can be injected into the yolk and its incorporation by the proliferating cells can then be measured by performing immunohistochemistry on fixed embryos at different developmental stages using an anti-BrDU antibody. By subjecting zebrafish embryos to this treatment while quantifying BrDU incorporation by tailbud resident cells, one can imagine at least three distinct possible outcomes:

- **i.** Tailbud outgrowth is completely impaired in embryos treated with DNA replication inhibitors – demonstrating that cell proliferation is essential for tailbud outgrowth;
- **ii.** Tailbud outgrowth still occurs in embryos treated with DNA replication inhibitors, but the process is much slower when compared to DMSO-treated embryos and/or the embryos display a set of posterior body abnormalities – suggesting that cell proliferation is required, but it is not the only process involved in tailbud outgrowth;
- **iii.** Tailbud outgrowth in embryos treated with DNA replication inhibitors occurs normally as in control DMSO-treated embryos – indicating that cell proliferation is not at all required for tailbud outgrowth, a scenario that is less likely to be true and is not consistent with our preliminary results.

Based on the library of clones so far generated by RCA and on our experiments using the Cecyil zebrafish transgenic line, we strongly believe that cell proliferation in lineage-restricted progenitors throughout the posterior body is one of the mechanisms that enables posterior body elongation in zebrafish. Therefore by performing these experiments we would expect to observe at least a partial impairment in tailbud elongation accompanied by a slow BrDU uptake in tailbud cells.

Another important aspect that should be addressed in the future has to do with the conservation of the evolutionary mechanisms involved in the control of vertebrate

posterior body formation. Although it has been previously demonstrated that in avians (Catala *et al*., 1995) and *Xenopus* (Gont *et al*., 1993) the formation of the posterior body seems to rely mainly on the same mechanisms that are responsible for regulating morphogenesis and patterning more rostrally in the embryo, for other animal models such as mouse and zebrafish this is not yet clear. In these models, evidence of developmental features were found to be congruent with both Holmdahl's and Vogt's ideas, leading some authors to believe that these vertebrate species have a heterogenous tailbud (Handrigan, 2003). From an evolutionary point of view, it seems reasonable to infer that the common ancestor of all vertebrates must have had a heterogenous tailbud, a developmental trait that throughout evolution was maintained in some clades and at the same time lost in other groups where the formation of the posterior body evolved in a specialized fashion due to distinct selective pressures. This assumption got strengthen when Schubert *et al.* 2001 reached a similar conclusion upon studying the expression pattern of *Wnt* genes in the developing tailbud of amphioxus, which is considered to be the closest living proxy to the common ancestor of all vertebrates. Although a substantial amount of evidence point towards this scenario, further research addressing these issues is needed in order to understand how these developmental mechanisms differ between chordates *vs.* non-chordates and amniotes *vs*. anamniotes.

V.3. Future Perspectives

In the future more experiments addressing the molecular and cellular mechanisms involved in the regulation of tailbud outgrowth ought to be performed, aiming to:

1. Analyze the cell behaviours underlying the alterations in segment shape and size observed at the tissue level using live imaging;
2. Investigate in more detail the importance of notochord inflation and myogenesis for posterior body elongation;
3. Confirm the importance of cell proliferation during posterior body elongation and the (non-)existence of tailbud resident stem cells in zebrafish;
4. Perform complementary studies in other animal models, including amniotes and other anamniotes such as amphioxus, in order to conduct a comparative study aiming to evaluate the (non-)conservation of the evolutionary mechanisms underlying tailbud outgrowth in vertebrates.

References

Agathon, A., Thisse, C. and Thisse, B. (2003). The molecular nature of the zebrafish tail organizer. Letters to Nature **424**, 448-452.

Blanchard, G. B., Kabla, A. G., Schultz, N. L., Butler, L. C., Sanson, B., Gorfinkiel, N., Mahadevan, L. and Adams R. J. (2009). Tissue tectonics: morphogenetic strain rates, cell shape change and intercalation. Nat. Methods **6**, 458-464.

Boehm, B., Westerberg, H., Lesnicar-Pucko, G., Raja, S., Rautschka, M., Cotterell, J., Swoger, J. and Sharpe, J. (2010). The role of spatially controlled cell proliferation in limb bud morphogenesis. PLoS Biology 7(8): e1000420.

Bouldin, C. M., Snelson, C. D., Farr III, G. H. and Kimelman, D. (2014). Restricted expression of cdc25a in the tailbud is essential for formation of the zebrafish posterior body. Genes & Dev. **28**, 384-395.

Catala, M., Teillet, M. A. and Le Douarin, N. M. (1995). Organization of the tailbud analyzed with the quail-chick chimaera system. Mech. Dev. **51**, 51-65.

Cooper, K. L., Oh, S., Sung, Y., Dasari, R. R., Kirschner, M. W. and Tabin, S. J. (2013). Multiple phases of chondrocyte enlargement underlie differences in skeletal proportions. Nature **495**, 375-378.

Economou, A., Brock, L., Cobourne, M. and Green, J. (2013). Whole population cell analysis of a landmark-rich mammalian epithelium reveals multiple elongation mechanisms. Development **140**, 4740-4750

Gong, Y., Mo, C. and Fraser, S. E. (2004). Planar cell polarity signalling controls cell division orientation during zebrafish gastrulation. Letters to Nature **430**, 689-693.

Gont, L. K., Steinbeisser, H., Blumberg, B. and De Robertis, E. M. (1993). Tail formation as a continuation of gastrulation: The multiple cell populations of the Xenopus tailbud derive from the late blastopore lip. Development **119**, 991-1004.

Handrigan, G. (2003). Concordia discors: duality in the origin of the vertebrate tail. J. Anat**. 202**, 255-267.

Hoffman, S., Psaltis, P., Clark, K., Spoon, D., Chue, C., Ekker, S. and Simari R. (2014). An in vivo method to quantify lymphangiogenesis in zebrafish. Plos One **7**(9): e45240.

Holmdahl, D.E. (1925). Experimentelle untersuchungen uber die lage der grenze primarer und sekundarer korperentwicklung beim huhn. Anat. Anz. **59**, 393-396.

Kanki, J. P. and Ho, R. K. (1997). The development of the posterior body in zebrafish. Development **124**, 881–893.

Keller, R. (2002). Shaping the vertebrate body plan by polarized embryonic cell movements. Science **298**, 1950-1954.

Keller, R. (2006). Mechanisms of elongation in embryogenesis. Development **133**, 2291-2302.

Kinder, S. J., Tsang, T. E., Quinlan, G. A., Hadjantonakis, A. K., Nagy, A. and Tam P. P. (1999). The orderly allocation of mesodermal cells to the extraembryonic structures and the anteroposterior axis during gastrulation of the mouse embryo. Development, **126** 4691–4701

Kimmel, C. B., Warga, R. M. and Schilling, T. F. (1990). Origin and organization of the zebrafish fate map. Development **108**, 581-94.

Kimmel, C. B., Ballard, W. W., Kimmel, S. R., Ullmann, B. and Schilling, T. F. (1995). Stages of embryonic development of the zebrafish. Dev. Dyn. **203**, 253-310.

Montero, J. A. and Heisenberg, C. P. (2004). Gastrulation dynamics: cells move into focus. Trends in Cell Biology **14**, 620-627.

Mosimann, C., Kaufman, C. K., Li, P., Pugach, E. K., Tamplin, O. J. and Zon, L. I. (2011). Ubiquitous transgene expression and Cre-based recombination driven by the ubiquitin promoter in zebrafish. Development **138**, 169-177.

Nicolas, J.F., Mathis, L. and Bonnerot, C. (1996). Evidence in the mouse for self-renewing stem cells in the formation of a segmented longitudinal structure, the myotome. Development **122**, 2933-2946.

Pasteels, J. (1943). Proliferations et croissance dans la gastrulation et la formation de la queue des vertebres. Arch. Biol. **54**, 1-51.

Petit, A. C., Legué, E. and Nicolas, J.F. (2005). Methods in clonal analysis and applications. Reprod. Nutr. Dev. **45**, 321–339.

Robles, V., Martí, M. and Belmonte, J. (2011). Study of pluripotency markers in zebrafish embryos and transient embryonic stem cell cultures. Zebrafish. **8**(2): 57–63.

Roth, V. L. and Mercer, J. M. (2000). Morphometrics in development and evolution. Amer. Zool. **40**(5): 801–810.

Sepich, D. S. and Solnica-Krezel L. (2005). Analysis of cell movements in zebrafish embryos: morphometrics and measuring movement of labeled cell populations in vivo. Methods Mol Biol. **294**, 211-33

Shih, J. and Fraser, S. E. (1995). Distribution of tissue progenitors within the shield region of the zebrafish gastrula. Development **121**, 2755-2765.

Schubert, M., Holland, L. Z., Stokes, M. D. and Holland, N. D. (2001). Three amphioxus Wnt genes (AmphiWnt3, AmphiWnt5, and AmphiWnt6) associated with the tailbud: The evolution of somitogenesis in chordates. Dev. Biol. **240**, 262-273.

Sugiyama, M., Sakaue-Sawano, A., Iimura, T., Fukami, K., Kitaguchi, T., Kawakami, K., Okamoto, H., Higashijima, S-i. and Miyawaki, A. (2009). Illuminating cell-cycle progression in the developing zebrafish embryo. Proc. Natl. Acad. Sci. USA **49**, 20812-20817.

Tzouanacou, E., Wegener, A., Wymeersch, F. J., Wilson, V. and Nicolas, J. F. (2009). Redefining the progression of lineage segregations during mammalian embryogenesis by clonal analysis. Developmental Cell **17**, 365–376.

Westerfield, M. (1993). The Zebrafish Book. A Guide for the Laboratory Use of Zebrafish. Eugene, OR: Univesity of Oregon Press.

Wolpert, L. (2010). Arms and the man: the problems of symmetric growth. PLoS Biology 8(9): e1000477.

Zhang, L., Kendrick, C., Jülich, D. and Holley, S. A. (2008). Cell cycle progression is required for zebrafish somite morphogenesis but not segmentation clock function. Development **135**, 2065-2070.

Appendix I – Supplementary data

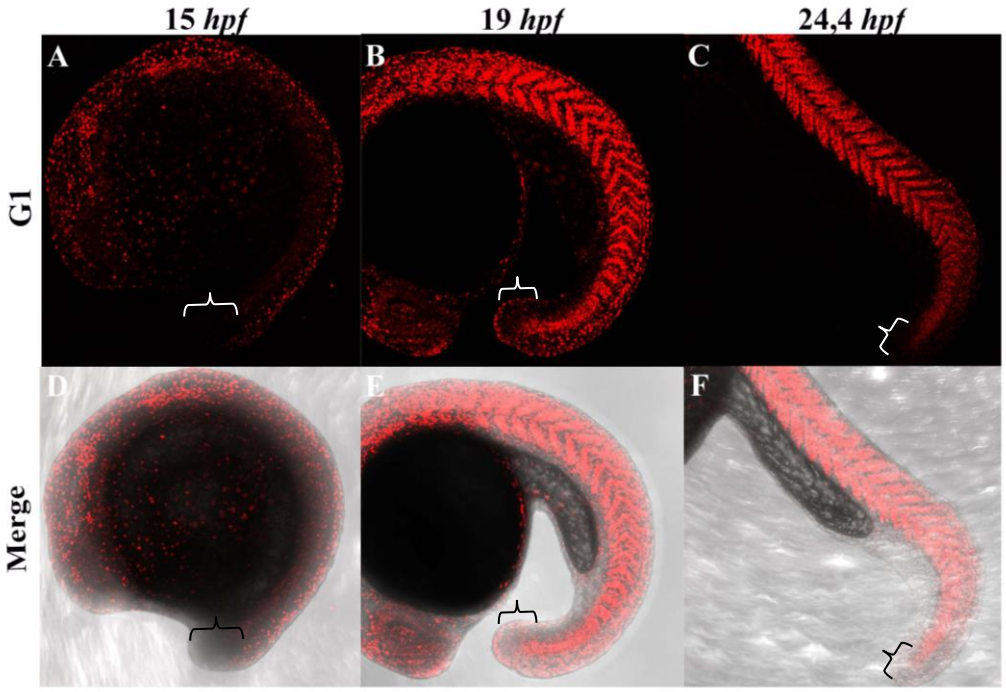

Figure S1. Post-mitotic cells progressively invade the posterior body. Representative maximum intensity projection of PFA-fixed Cecyil embryos during posterior body formation, visualizing post-mitotic non-proliferating cells (red; **A-C**). Developmental stages are expressed in *hpf*. Z-stacks were acquired from live embryos using a Leica SP5 confocal microscope equipped with an objective lens (x10 N.A. 0.3). Panels **(D-F)** represent a single bright field plane merged with the green signal to better visualize the embryonic structures. Brackets delimit the tailbud region. The presence of differentiated cells undergoing G1 is relatively low **(red; A, D).** As the embryo grows, the red signal increases significantly and strongly highlightswell-differentiated cells, such as post-mitotic muscle cells at the level of the somites **(B, C, E and F)**. Brackets delimit the tailbud region.

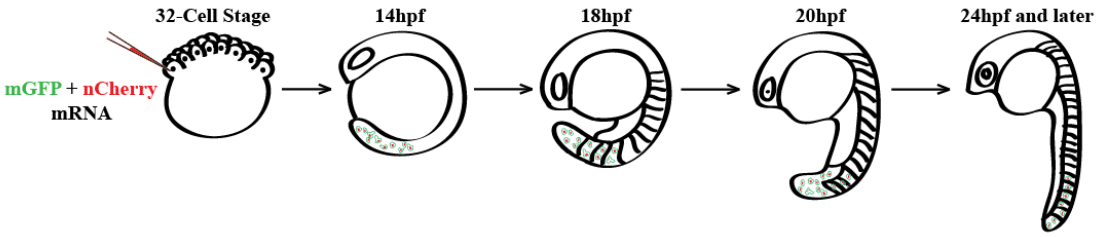

Figure S2. Schematic figure of the generation of mosaically labeled embryos injected with membrane eGFP and nuclear mCherry mRNA's at the 32-cell stage. The developmental stages in *hpf* are indicated above.